Mannose 6-Phosphate/Insulin-like Growth Factor–II Receptor Targets the Urokinase Receptor to Lysosomes via a Novel Binding Interaction

Anders Nykjær,* Erik I. Christensen,‡ Henrik Vorum,* Henrik Hager,* Claus M. Petersen,* Hans Røigaard,* Hye Y. Min,§ Frederik Vilhardt,‖ Lisbeth B. Møller,¶ Stuart Kornfeld, and Jørgen Gliemann***

*Department of Medical Biochemistry, ‡Department of Cell Biology, University of Aarhus, DK-8000 Aarhus, Denmark; §Chiron Corporation, Emeryville, California; ‖Department of Anatomy, Panum Institute, University of Copenhagen, Denmark; ¶John F. Kennedy Institute, Copenhagen, Denmark; and **Division of Hematology-Oncology, Washington University, St. Louis, Missouri

Abstract. The urokinase-type plasminogen activator receptor (uPAR) plays an important role on the cell surface in mediating extracellular degradative processes and formation of active TGF-β, and in nonproteolytic events such as cell adhesion, migration, and transmembrane signaling. We have searched for mechanisms that determine the cellular location of uPAR and may participate in its disposal. When using purified receptor preparations, we find that uPAR binds to the cation-independent, mannose 6-phosphate/insulin-like growth factor–II (IGF-II) receptor (CIMPR) with an affinity in the low micromolar range, but not to the 46-kD, cation-dependent, mannose 6-phosphate receptor (CDMPR). The binding is not perturbed by uPA and appears to involve domains DII + DIII of the uPAR protein moiety, but not the glycosylphosphatidylinositol anchor. The binding occurs at site(s) on the CIMPR different from those engaged in binding of mannose 6-phosphate epitopes or IGF-II. To evaluate the significance of the binding, immunofluorescence and immunoelectron microscopy studies were performed in transfected cells, and the results show that wild-type CIMPR, but not CIMPR lacking an intact sorting signal, modulates the subcellular distribution of uPAR and is capable of directing it to lysosomes. We conclude that a site within CIMPR, distinct from its previously known ligand binding sites, binds uPAR and modulates its subcellular distribution.

THE urokinase-type plasminogen activator receptor (uPAR)[1] present on the surface of most cell types is a key component in the control of cell adhesion, migration, and extracellular proteolysis (for reviews see Fazioli and Blasi, 1994; Andreasen et al., 1997, Chapman, 1997). The recently discovered function as an adhesion molecule is mediated by binding of domains DII + DIII of the three domain uPAR to the extracellular matrix protein vitronectin in a reaction facilitated by binding of urokinase (uPA) to the NH_2-terminal DI (Wei et al., 1994). In addition, uPAR and two integrins can form stable complexes that promote uPAR binding to vitronectin and concomittantly suppress the normal adhesive functions of the integrins (Wei et al., 1996). The balance between cell adhesion and cell detachment is primarily governed by the type-1 plasminogen activator inhibitor (PAI-1), which competes with uPAR (Deng et al., 1996; Kanse et al., 1996) and with integrins (Stefansson and Lawrence, 1996; Kjøller et al., 1997) for binding to vitronectin.

The established importance of uPAR in pericellular proteolysis is due to its avid binding of single chain pro-uPA to domain DI followed by activation to the two chain uPA, which in turn activates plasminogen. The uPA-catalyzed plasminogen activation is much faster in the presence than in the absence of cells because of the cell surface receptor association of both uPA and plasminogen (Ellis et al., 1989; Bugge et al., 1995). Similarly, uPAR is necessary for efficient uPA and plasmin-mediated activation of latent TGF-β on the cell surface (Rifkin et al., 1993; Ode-

Address all correspondence to Anders Nykjær, Department of Medical Biochemistry, University of Aarhus, Ole Worms Allé, Bldg. 170, DK-8000 Aarhus C, Denmark. Tel.: +45 89422884. Fax: +45 86131160. E-mail: an@biokemi.aau.dk

1. *Abbreviations used in this paper*: Asp-N, asparaginase-N; CDMPR, cation-dependent mannose 6-phosphate receptor; CIMPR, cation-independent mannose 6-phosphate/insulin-like growth factor–II receptor; DTSSP, 3,3-dithiobis(sulfosuccinimidylproprionate); Glc-6-P, glucose 6-phosphate; GPI, glycosylphosphatidylinositol; IGF-II, insulin-like growth factor–II; LAMP-1 and -2, lysosomal associated membrane protein 1 and 2; LDL, low density lipoprotein; LRP, LDL receptor–related protein; Man-6-P, mannose 6-phosphate; m-uPAR, mouse uPAR; PiPLC, phosphoinositol-specific phospholipase C; RAP, receptor-associated protein; TGF-β, transforming growth factor–β; uPAR, urokinase-type plasminogen activator receptor.

kon et al., 1994). The activity of uPA bound to uPAR is quenched by inhibitors, particularly PAI-1, which therefore holds a central position in suppressing both the uPAR-mediated cell adhesion and the pericellular proteolysis. Recently, an alternative role of uPAR in fibrinolysis was demonstrated since the uPAR-dependent binding to vitronectin promotes binding to and degradation of fibrin, mediated by the leucocyte integrin Mac-1 in a reaction inhibited by uPA (Di et al., 1996).

Although it is glycosylphosphatidylinositol (GPI) anchored and devoid of transmembrane and cytoplasmic domains, uPAR is also endowed with transmembrane signaling properties thought to involve an association with an unknown adaptor molecule and activation of tyrosine kinases of the Src family of proteins (Bohuslav et al., 1995). Stimulation of chemotaxis has been observed using uPA derivatives with receptor-binding properties but devoid of catalytic activity (Busso et al., 1994). When released by proteolytic cleavage, the NH_2-terminal domain DI can induce chemotaxis, and it was proposed that both binding of uPA to DI and proteolytic release of DI induce conformational changes in the domain that unmask epitopes required for the adaptor-mediated signaling (Resnati et al., 1996). Interestingly, a uPAR fragment containing only DII + DIII is present on the surface of different cell lines, demonstrating that DI can be cleaved off in cells (Solberg et al., 1994), and it has been reported that uPA itself can cleave uPAR between DI and DII (Høyer-Hansen et al., 1992).

uPAR is, in an interplay with the other components of the uPA system, capable of enhancing cell migration and invasion via proteolytic and non-proteolytic mechanisms, and increased expression of uPAR is a poor prognostic marker in several cancerous diseases (Andreasen et al., 1997). This suggests that the expression of uPAR should be subject to a tight regulation and that mechanisms for its disposal should be available. It has been shown that PAI-1, after the formation of a stable ternary complex with uPAR-bound uPA (Nykjær et al., 1994*a*), induces the internalization of the entire complex via the endocytic low density lipoprotein (LDL) receptor related protein (LRP)/α_2-macroglobulin receptor (Conese et al., 1995). The uPA and PAI-1 moieties are transferred to lysosomes for degradation (Cubellis et al., 1990; Estreicher et al., 1990; Jensen et al., 1990), whereas uPAR is recycled back to the cell surface (Nykjær et al., 1997). Since uPAR reappearing on the cell surface is capable of binding new ligand, the recycling allows the cell to switch between different uPAR functions depending on the pericellular milieu. In addition, the LRP-mediated internalization causes a decrease in the steady-state concentration of uPAR on the cell surface. Accordingly, it was recently shown that cells deficient in LRP because of targeted gene disruption exhibited increased uPAR on the cell surface and increased migration velocity in vitronectin-coated wells (Weaver et al., 1997). However, the recycling mediated by LRP does not provide a mechanism for disposal of uPAR, and we have therefore searched for other mechanisms that might modulate the distribution and fate of uPAR in cells.

Here we show that uPAR binds to the 275-kD cation-independent mannose 6-phosphate (Man-6-P)/insulin-like growth factor–II receptor (CIMPR) via an interaction not involving Man-6-P residues. CIMPR is a multifunctional receptor present in the Golgi apparatus, on the cell membrane and in endosomes of most cell types. It targets newly synthesized Man-6-P containing lysosomal acid hydrolases from the TGN to late endosomes, mediates endocytosis of insulin-like growth factor–II (IGF-II) and participates in the activation of latent TGF-β (for review see Kornfeld, 1992). We demonstrate that the binding of uPAR to CIMPR is independent of uPA, and that the binding epitope on CIMPR is different from those binding Man-6-P and IGF-II. Finally, we show that CIMPR modulates the subcellular distribution of uPAR and is capable of directing it to lysosomes.

Materials and Methods

Reagents

Glucose 6-phosphate (Glc-6-P), mannose 6-phosphate, and *N*-propyl-galleat, leupeptin, and pepstatin A were from Sigma Chemical Co. (St. Louis, MO), and $Na^{125}I$, D-[2-^{3}H]mannose, and Pro-mix (L-[^{35}S]methionine and L-[^{35}S]cysteine) were from Amersham International (Little Chalfont, UK). CNBr-activated Sepharose was purchased from Pharmacia Biotech Sevrage (Uppsala, Sweden), phosphoinositol-specific phospholipase C (PiPLC), Asparaginase-N (Asp-N), and IGF-II were from Boehringer Mannheim GmbH (Mannheim, Germany), and 3,3-dithiobis(sulfosuccinimidylproprionate) (DTSSP) was from Pierce Chemical Co. (Rockford, IL). β-Glucuronidase was purified from the secretions of 13.2.1 cells (a gift of Dr. W. Sly, St. Louis University, St. Louis, MO) as described previously (Jadot et al., 1992). Recombinant receptor–associated protein (RAP) was prepared as described (Nykjær et al., 1992). Specific rabbit anti–human uPAR IgG was purified by affinity chromatography using immobilized recombinant uPAR. Rabbit anti-CIMPR antibodies were raised against bovine CIMPR and purified on protein A–Sepharose (Pharmacia Biotech Sevrage). Monoclonal anti–human uPAR IgG, clones R2, and R4, were gifts from Dr. E. Rønne (Finsen Institute, Copenhagen, Denmark), and rabbit anti–human, lysosomal-associated membrane protein (LAMP)-1 and rat anti–mouse LAMP-2 antibodies were generously provided by Dr. S. Carlsson (University of Umeå, Umeå, Sweden) and Dr. I. Mellman (Yale University School of Medicine, New Haven, CT), respectively. Texas red–conjugated goat anti–mouse IgG and Fluoromount were from Southern Biotechnology Associates (Birmingham, AL), and FITC-labeled swine anti–rabbit IgG was from DAKOPATTS (Copenhagen, Denmark). Goat anti–rabbit gold and goat anti–rat gold were from BioCell (Cardiff, UK), and streptavidin-gold was purchased from Zymed Labs, Inc. (South San Francisco, CA).

Cell Lines

Murine L cells lacking CIMPR (clone D9) and L cells transfected with full-length CIMPR (clone Cc2) and a truncated receptor lacking 154 amino acids of the cytoplasmatic tail (clone Dd4) have been described before (Lobel et al., 1989). The D9 cell line transfected with a mutated CIMPR lacking intact Man-6-P binding sites (clone Mut39, Arg^{435} to Ala and $Arg^{1,334}$ to Ala) (Dahms et al., 1993) was generously provided by Dr. N.M. Dahms, Medical College of Wisconsin (Milwaukee, WI). The D9 cell line transfected with the 46-kD, cation-dependent mannose 6-phosphate receptor (CDMPR) has been described (Johnson et al., 1990).

Mouse LB6 clone 19 cells expressing human wild-type uPAR have been described previously (Roldan et al., 1990). LB6 cells transfected with a chimeric receptor (uPAR-TM) encoding human uPAR terminated with the transmembrane segment of the EGF receptor were constructed as follows: base pairs 2,113–2,223 of the EGF-receptor gene (these sequence data are available from GenBank/EMBL/DDBJ under accession No. X00588) was amplified by PCR. The PCR primers (5′-ACG AAT GGG CCT GAT ATC CCG TCC ATC GCC-3′ and 5′-C CCT CTC CTG GAG CTC CCT CTA CAG CGT GCG CTT-3′) contained recognition sequences for EcoRV and SacI, respectively. The downstream primer was designed to encode a UAG termination codon. The amplified fragment was substituted for the COOH-terminal EcoRV–SacI fragment from p-S-uPAR1 (Masucci et al., 1991) giving rise to plasmid p-TM-uPAR1. This plasmid thus encodes a fusion protein consisting of the first 277 amino acids of uPAR fused to a 37–amino acid transmembrane segment

derived from the EGF receptor (IPSIATGMVGALLLLLVVALGI-GLFMRRRHIVRKRTL-STOP). LB6 cells were transfected with p-TM-uPAR1 by the calcium phosphate coprecipitation method, as described previously (Møller et al., 1992). Expression of the encoded protein was verified by cross-linking experiments to ^{125}I-labeled, NH_2-terminal fragment of uPA and resistance to treatment with PiPLC.

HeLa cells were from American Type Culture Collection (Rockville, MD). All cell lines were cultured according to standard procedures.

Purification of Receptors

Soluble CIMPR was purified from FCS by phosphomannosyl–Sepharose affinity chromatography essentially as described (Ludwig et al., 1991). Material eluting from the column was dialyzed twice against buffer A (10 mM Hepes, 2 mM $CaCl_2$, 1 mM $MgCl_2$, 140 mM NaCl) adjusted to pH 5.2 followed by two times dialysis against buffer A at pH 7.4. The receptor was finally concentrated on Centricon 100 (Amicon Corp., Danvers, MA) and frozen at −200°C in the presence of glycerol. Purification of full-length CIMPR from bovine and chicken liver was performed as described (Hoflack and Kornfeld, 1985).

uPAR purified from U937 cells by antibody affinity chromatography (Mizukami et al., 1991) was provided by R.F. Todd III (University of Michigan Medical Center, Ann Arbor, MI). After radiolabeling of the receptor using the chloramine-T method to obtain ~4×10^{16} becquerel/mol, the receptor preparation was further purified by affinity chromatography on DFP-uPA coupled to CNBr-activated Sepharose, ensuring >98% purity of the preparation. Metabolically labeled uPAR was purified from different cell types by immunoprecipitation. In brief, labeled cells were loosened from the culture flasks by incubation with 10 mM EDTA for 10 min at 20°C, washed, and then lysed on ice in 50 mM Tris-HCl, 10 mM EDTA, 1 mM PMSF, 1% Triton X-114, pH 8.1. The lysate was cleared by centrifugation at 4°C and the detergent phase enriched in uPAR was collected by incubation at 37°C (5 min) and centrifugation. The extract was washed twice in 0.1 M Tris-HCl, pH 8.1, and the detergent phase was finally reconstituted in buffer A, pH 7.2, containing 0.5% CHAPS (Boehringer Mannheim) to inhibit further micelle formation (Nykjær et al., 1994*b*). Solubilization of chimeric uPAR containing the transmembrane domain of the EGF receptor was done in the buffer containing Triton X-100. In some experiments, the detergent phase separation of the Triton X-114 lysates was substituted by washing of the cells with buffer A, pH 7.2, and treatment with 0.4 μg/ml Asp-N or 0.7 U/ml PiPLC for 3 h to release uPAR from the cell membrane. The medium was next made 1% with respect to Triton X-100, and BSA, 10 mM EDTA, and 1 mM PMSF were added. The receptors were subsequently purified by immunoprecipitation as follows. Detergent phases and medium containing soluble uPAR were precleared by incubation with 50 μl mock-coupled CNBr-Sepharose/ml suspension for 4 h at 4°C. The preabsorbed supernatants were subsequently incubated for 4 h at 4°C with 50 μl CNBr-Sepharose coupled with affinity-purified rabbit anti-uPAR IgG. The Sepharose was washed twice in MB-buffer, 0.1% Triton X-100, pH 7.3, and then two times in the same buffer containing 0.8 M NaCl, and finally three times in the initial buffer. Bound radioactive receptor was released from the Sepharose beads by incubation in 0.1 M glycine, 0.1% Triton X-100 for 10 min on ice, and the eluate was finally neutralized by the addition of 1/40 volume Tris-base, pH 9.0. As determined by SDS-PAGE and fluorography, the uPAR preparations were >90% pure. uPAR expression in baculovirus has been described before (Wei et al., 1996) as well as purification and iodination of LRP (Moestrup and Gliemann, 1991; Nykjær et al., 1993).

Affinity Chromatography

CIMPR, LRP, and RAP were covalently immobilized on CNBr-Sepharose according to the manufacturers directions at a concentration of 5–6 mg/ml gel, and columns were packed with 1–2 ml of the respective affinity matrices. The columns were equilibrated in buffer A containing 0.1% BSA and 0.25% Tween-20, pH 7.2. About 75,000 cpm labeled uPAR in 2 ml buffer were incubated simultaneously on each column for 2 min at 20°C. The eluted fractions were collected and reapplied to the columns. Each incubation was repeated four times corresponding to a total incubation time of 8 min. The affinity matrices were next washed four times with 5 ml binding buffer followed by 2 × 5 ml buffer containing 5 mM Glc-6-P, and then with 3 × 5 ml buffer containing 5 mM Man-6-P. The columns were finally eluted with 4 × 5 ml 0.1 M glycine, 0.25% CHAPS, pH 2.7. The radioactivity in the various 5-ml fractions was determined and the recovery of material applied to each column was calculated.

Real Time Interaction Analysis

The studies were performed using a BIAcore 2000 apparatus (Pharmacia Biotech Sevrage, Uppsala, Sweden). Pro-uPA was immobilized on a carboxymethyl-type CM5 sensor chip as described previously (Behrendt et al., 1996) using the Amine Coupling Kit supplied by the manufacturer. For further explanation, see legend to Fig. 4 *A*.

Dialysis Exchange

Binding of ^{125}I-uPAR to CIMPR in solution was performed as described by Pedersen et al. (1986). Each dialysis chamber contained 20 μl solution separated by a cellulose ester membrane with a cut off at M_r ~100,000. In separate experiments, the rate of diffusion was found to be proportional to the uPAR concentration. To determine binding of uPAR at low concentration, thermostated solutions (4°C) of CIMPR (3 μM) and recombinant soluble uPAR expressed in baculovirus (25 pM) were injected on both sides of the membrane, including a small fraction of ^{125}I-uPAR on the left side only. Initial experiments showed no difference between binding of ^{125}I-labeled, wild-type uPAR purified from U937 cells and ^{125}I-labeled uPAR expressed in baculovirus. The radioactivity in the compartments were determined at 50–100 min, i.e., before the equilibrium of the tracer was achieved (~300 min). The following equation (Pedersen et al., 1986) was used for calculation:

$$\ln (Q_{\text{left}} - Q_{\text{right}} / Q_{\text{left}} + Q_{\text{right}}) = -c \times k_0 \times t / C, \quad (1)$$

where Q denotes radioactivity after dialysis for minutes (t), C is the total concentration of uPAR (bound + unbound), and c is the concentration of unbound uPAR. The rate constant, k_0, was determined in experiments without CIMPR, in which case $c = C$ in Eq. 1. The concentration of bound uPAR (C–c) was then expressed in per cent of the total uPAR concentration. To assess the binding stoichiometry, unlabeled recombinant uPAR was added at varying concentrations to both sides of the dialysis membrane (up to 38 μM), and the CIMPR concentration was raised to 25 μM. In some cases, K_d was calculated from microdialysis experiments with only one low uPAR concentration using the approximation:

$$Kd = c \times [\text{CIMPR}] / (C - c), \quad (2)$$

where [CIMPR] is the CIMPR concentration.

Metabolic Labeling and Cross-linking

Cells were grown to 75% confluence, washed twice in medium lacking methionine and cysteine, and then incubated for 24 h in cysteine/methionine-depleted medium containing 10% normal medium, 10% fetal calf serum dialyzed against phosphate buffered saline and 35 μCi/ml Pro-mix. The cells were next washed and chased for 30 min in complete medium enriched in methionine and cysteine (10 times excess), loosened from the culture flasks by incubation with PBS containing 10 mM EDTA, and then washed three times in PBS, pH 7.4. In some experiments cells were labeled with D-[2-^{3}H]mannose as described (Brunetti et al., 1994). For purification of metabolically labeled receptors, the cells were lysed and the receptor isolated using immunoprecipitation as described in a previous paragraph. Cross-linking experiments were performed as follows. The labeled cells resuspended in PBS were incubated in the absence or presence of 5 mM Man-6-P for 2 h on ice. The cell suspensions were then treated with 2 mM of the bifunctional and reducible cross-linker DTSSP for 30 min on ice. The cross-linking reaction was subsequently quenched by the addition of 50 mM Tris-HCl, pH 7.4, followed by further incubation for 30 min. Finally, the cells were lysed in 50 mM Tris-HCl, 10 mM EDTA, 1 mM PMSF, 1% Triton X-100, pH 7.4, and the lysates were cleared by centrifugation.

Cross-linked uPAR/CIMPR complexes were isolated by precipitation using anti-uPAR IgG Sepharose followed by elution and reimmunoprecipitated by incubation for 4 h at 4°C with rabbit anti-CIMPR, IgG-coupled Sepharose. The Sepharose was washed as described above and bound radioactivity was released by incubation with 0.1 M glycine, 0.1% Triton X-100, pH 2.7, for 10 min on ice. The eluate was neutralized, boiled in the presence of 20 mM dithioerythritol, analyzed by 4–16% SDS-PAGE, and then applied to fluorography according to standard procedures.

Immunofluorescence Microscopy

Subconfluent HT1080 cells, clone D9, Cc2, Dd4, Mut 39, or ML4 cells

were washed once in PBS and fixed for 15 min at 20°C in PBS containing 2% formaldehyde. The cells were washed twice in PBS and nonspecific binding was blocked by incubation for 15 min with 10% goat serum in PBS containing 0.2% saponin for cell permeabilization. Clones D9, Cc2, Dd4, Mut39, and ML4 cells were incubated with affinity-purified rabbit anti-uPAR IgG and HT1080 cells with a rabbit antibody to LAMP-1 for 45 min followed by 2 × 5 min wash in PBS containing 0.1% Triton X-100. Secondary FITC-conjugated swine anti–rabbit antibody was then applied for 30 min and the cells were again washed for 2 × 5 min. For HT1080 cells a second round of immunodetection was performed using the monoclonal antibody R2 against uPAR followed by Texas red–labeled goat anti–mouse IgG. Finally, the cells were rinsed briefly in distilled water, the coverslips mounted with Fluoromount containing 2.5 mg/ml *N*-propyl-gallate and the cells viewed in an Olympus OM 50 microscope equipped with epifluorescence.

Immunoelectron Microscopy

Approximately 5.0 × 10^6 cells from clones D9, Cc2, Dd4, Mut 39, and ML4 were either fixed directly or treated for 17 h with 50 μg/ml leupeptin and 67 μg/ml pepstatin A before fixation. The cells were fixed in 2% formaldehyde, 0.1 M sodium cacodylate buffer, pH 7.2, for up to 18 h, embedded in 15% gelatin, and then infiltrated with 2.3 M sucrose containing 2% formaldehyde for 30 min, and frozen in liquid nitrogen. Ultrathin cryosections, 70–90 nm, were obtained with a FCS Ultracut S cryoultramicrotome (Reichert-Jung, Vienna, Austria) at ~−100°C and collected on 300 mesh Ni grids. The sections were incubated overnight at 4°C with affinity-purified polyclonal rabbit anti-uPAR IgG (5 μg/ml), and then with 10-nm goat anti–rabbit gold or, for double labeling, 5-nm goat anti–rabbit gold at 4°C for 2 h. Double-labeling experiments were performed to demonstrate, in addition to uPAR, the lysosome-associated membrane protein LAMP-2 using a monoclonal rat anti–mouse antibody visualized by 10-nm goat anti–rat gold, or to demonstrate CIMPR using biotinylated affinity-purified rabbit anti–bovine CIMPR IgG and 10-nm streptavidin–gold. The sections were finally contrasted with methyl cellulose containing 0.3% uranylacetate (Tokuyasu, 1978; Griffiths et al., 1984) and studied in a Philips EM 208 or a Philips CM100 electron microscope (Philips Electron Optics, Mahwah, NJ). Controls incubated with either non-specific monoclonal antibodies, protein A affinity-purified rabbit immunoglobulin, preabsorbed polyclonal rabbit anti-uPAR IgG, or without primary antibody, showed no specific labeling at all.

The immunogold distribution over the cells, using affinity-purified rabbit anti-uPAR, was determined quantitatively as follows. Approximately 25 electron micrographs including as much cytoplasm and cell surface as possible from each of the five cell lines were taken at random at a primary magnification of ×11,500 and enlarged threefold. Gold particles were counted over the plasma membrane, over cytoplasmatic vacuoles and over the nucleus. The cytoplasmatic area analyzed in the five groups was determined by point counting. The total number of gold-particles counted was 6755. The background labeling, as determined by the number of gold-particles over the nuclei was very low, range 0.4–1.1 gold particles/μm^2.

Results

We initially wanted to elucidate the intracellular location of uPAR in unchallenged cells in view of the previous observation that the ternary uPAR/uPA/PAI-1 complex can be internalized in an LRP assisted process followed by recycling to the cell surface (Nykjær et al., 1997). Surprisingly, as shown in Fig. 1 (*left column*), incubation of human HT1080 fibroblasts with leupeptin and pepstatin A to inhibit lysosomal hydrolases resulted in significant perinuclear staining for uPAR in LAMP-1–positive vesicles compatible with lysosomes. To ascertain that the intracellular location of uPAR was not the result of internalization mediated by LRP, some incubations were performed in the presence of 400 nM RAP, which blocks the binding of uPAR-bound uPA–inhibitor complex to LRP (Nykjær et al., 1992) and to other members of the LDL receptor family (Heegaard et al., 1995). As shown in Fig. 1 (*right column*), the presence of RAP did not influence the staining pattern. We speculated that a receptor important in endocytosis and sorting, and not belonging to the LDL receptor family, might account for the apparent targeting of uPAR to lysosomes. We therefore performed affinity chromatography of solubilized membranes from HeLa cells using Sepharose-immobilized uPAR, and an ~275-kD protein, tentatively identified as CIMPR by Western blotting, was eluted at pH 2.7 together with several low molecular weight proteins (data not shown).

CIMPR Binds Purified uPAR Independent of Man-6-P

To analyze possible binding of uPAR to CIMPR, uPAR purified from U937 cells was ^{125}I labeled and incubated for 8 min at pH 7.2 on a column of Sepharose-immobilized, soluble CIMPR from FCS followed by washings. As shown in Fig. 2, only 60-65% of the labeled uPAR was recovered from the CIMPR column following elution at pH 7.2, whereas those fractions contained >94% of the radioactivity when using control RAP–Sepharose (Fig. 2), LRP–Sepharose, or incubation on the CIMPR column at pH 5.5 (data not shown). The addition of Glc-6-P or Man-6-P (5 mM) did not cause release of the labeled uPAR from the CIMPR column, whereas the bound radioactivity was largely recovered after acidification to pH 2.7 (Fig. 2). Overall, the recoveries of the radioactivity applied to the CIMPR and RAP columns were 98–99%. Control experiments demonstrated that 85% of the well-characterized CIMPR ligand β-glucuronidase, which has Man-6-P–containing, Asn-linked oligosaccharides, was retained on the CIMPR column and eluted by 5 mM Man-6-P, but not Glc-6-P (not shown). To determine the fraction of ^{125}I-uPAR that could be bound to CIMPR–Sepharose, the incubation was extended to 60 min, and 69% was bound and eluted at pH 2.7 under this condition (not shown). Moreover, reincubation of the run through fractions revealed that at least 89% of the ^{125}I-uPAR preparation could eventually be bound to the CIMPR column.

To analyze the nature of the binding, wild-type human uPAR preparations by human uPAR in which the GPI anchor was replaced by a transmembrane domain, and murine uPAR (m-uPAR) were purified from metabolically labeled cells. Fig. 3 *A* provides an overview of the uPAR domain structure and shows the cleavage sites for the enzymes used to release the receptor from the cell surface. Fig. 3 *B* documents the purity of the ^{125}I-labeled uPAR (compare with Fig. 2) and of ^{35}S-labeled uPAR preparations released by enzymatic treatment of HeLa cells and LB6 clone 19 transfectants, ^{35}S-labeled chimeric receptor (uPAR-TM) consisting of the extracellular protein moiety of uPAR linked to the transmembrane domain of the EGF receptor, and ^{35}S-labeled wild-type m-uPAR from L cells. It can be seen in Fig. 3 *B* that particularly HeLa cells also contained the truncated uPAR consisting of domains DII + DIII.

The uPAR and m-uPAR preparations were next subjected to CIMPR affinity chromatography as described in the legend to Fig. 2. As shown in Table I, 20–35% of the labeled uPAR released from the cells by PiPLC and of m-uPAR was retained on CIMPR–Sepharose after incubation for 8 min. The labeled uPAR and m-uPAR were eluted at pH 2.7, but not by the addition of 5 mM Man-6-P

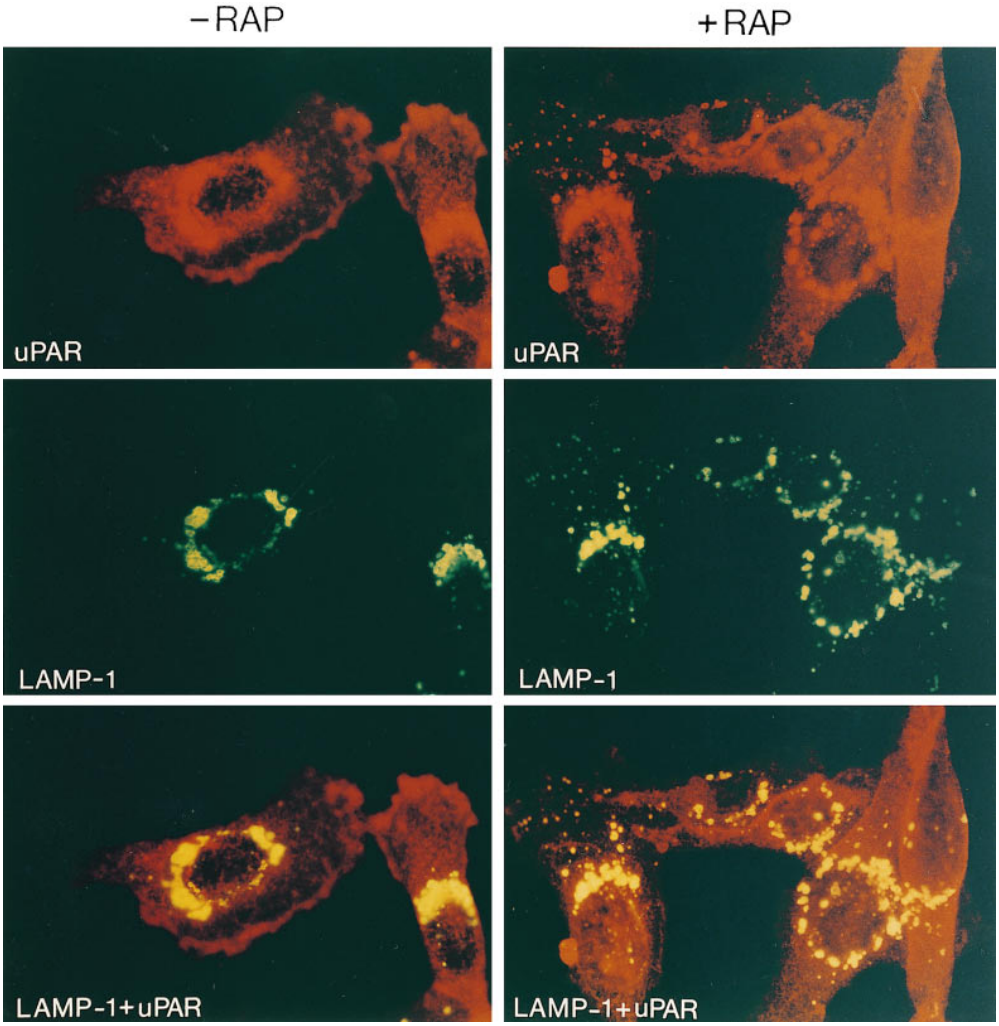

Figure 1. Labeling of uPAR in cultured fibroblasts. HT1080 fibroblasts were cultured in the presence of 50 μg leupeptin and 66 μg/ml pepstatin A for 17 h (*left panels*), or with 400 nM RAP for 12 h, followed by leupeptin and pepstatin A for 17 h in the continuous presence of RAP (*right panels*). The upper panels show uPAR labeling using the monoclonal anti-uPAR antibody R2 and rhodamine coupled goat anti–mouse IgG. The middle panels show LAMP-1 labeling using specific rabbit anti–LAMP-1 serum and FITC-labeled swine anti–rabbit IgG. The lower panels show a double exposure of the uPAR and LAMP-1 staining with colocalization appearing in yellow.

(or Glc-6-P). Similarly, other experiments (not shown) demonstrated 29% acid (but not Man-6-P) releasable binding to the CIMPR column of ^{125}I-labeled recombinant soluble uPAR expressed in baculovirus. The possible role of the GPI anchor was assessed by comparing the binding of uPAR released by PiPLC, which removes the lipid moiety, and by Asp-N, which releases the three protein domains from the entire glycolipid moiety (Fig. 3 *A*). As shown in Table I, removal of the GPI anchor had little effect and, moreover, uPAR-TM also bound to CIMPR. On the other hand, reduction and alkylation of uPAR released by PiPLC caused a marked reduction in binding suggesting that the overall conformation of the protein moiety is important. Control experiments (not shown) included parallel incubations on LRP and RAP–Sepharose columns that did not bind any of the uPAR preparations or m-uPAR.

These results strongly suggested that Man-6-P is not important for binding of uPAR to CIMPR, and this was confirmed by analysis of the carbohydrate moieties of uPAR. Carbohydrates contribute to 30–50% of the molecular size of uPAR, and we analyzed whether labeled Man-6-P was present in uPAR purified from HeLa cells incubated with [^{3}H]mannose (Brunetti et al., 1994). The results showed that binding to CIMPR could not depend on Man-6-P epitopes since 79% of the radioactivity was in complex-type oligosaccharides and 20.9% was in neutral high mannose oligosaccharides containing only a negligible fraction (0.1%) with one phosphomonoester and no detectable oligosaccharides with two phosphomonoesters (data not shown). When taken together, the results show that uPAR purified from several sources, as well as m-uPAR, can bind to CIMPR via epitopes different from Man-6-P and independent of the GPI anchor.

Stoichiometry of the Binding Reaction

Real time interaction analysis using a BIAcore instrument was performed to evaluate the affinity and stoichiometry of the binding. Initial experiments with uPAR immobilized directly to the sensor chip were unsuccessful. However, microdialysis experiments showed that uPA did not perturb the binding of uPAR to CIMPR (compare with Fig. 5). Pro-uPA, which binds uPAR with the same affinity as uPA, was therefore immobilized on the sensor chip followed by binding of uPAR. The amount of uPAR bound to the pro-uPA chip was calculated, and CIMPR was then applied. The analysis was performed in three flowcells: (*1*) with no coupling, (*2*) with immobilized pro-uPA alone, and (*3*) with pro-uPA plus associated uPAR. The BIA-

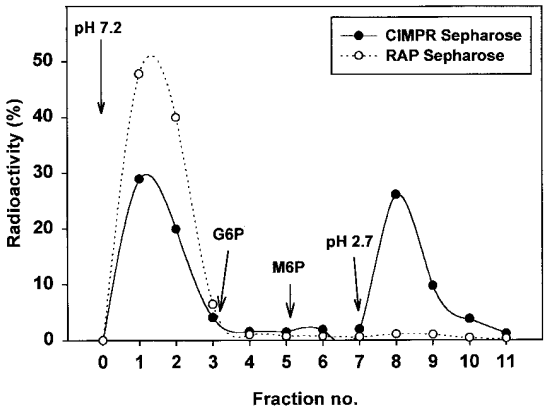

Figure 2. Binding of ^{125}I-labeled uPAR to immobilized CIMPR. uPAR purified from U937 cells and treated with PiPLC was iodinated, and ~75,000 cpm was applied to a column containing 1 ml Sepharose coupled with 5.4 mg CIMPR purified from FCS, followed by incubation for 8 min at 20°C. The filled symbols and solid line shows radioactivity eluted from the CIMPR column at pH 7.2 (3 × 5 ml fractions), followed by buffer containing 5 mM Glc-6-P (2 × 5 ml), 5 mM Man-6-P (3 × 5 ml), and 0.1 M glycine, 0.25% Tween-20, pH 2.7 (4 × 5 ml). The open symbols and dotted line show the result of a parallel control experiment using 1 ml Sepharose coupled with 5.5 mg recombinant purified RAP. The result is representative for one of five experiments using different CIMPR columns. The points show the radioactivity in per cent of the total radioactivity applied to the column and represent the mean values of triplicate determinations.

evaluation program was used for subtraction of the bulk effect of CIMPR measured in flowcell 1. The signal was identical in flowcells 1 and 2 indicating no binding of CIMPR to pro-uPA. The slow dissociation of uPAR from pro-uPA (Behrendt et al., 1996) was measured separately and was subtracted to compensate for drift of the baseline.

Fig. 4 *A* shows that CIMPR from FCS bound to immobilized uPAR expressed in baculovirus with a K_d ~1 μM (0.9–1.3 μM in five separate experiments). The calculated mole of CIMPR per mole of uPAR was 0.1 in the displayed experiments. Other experiments (not shown) confirmed that the binding was not inhibited by 5 mM Man-6-P. The inset documents the purity of the CIMPR preparation.

The quite low stoichiometry of CIMPR binding to uPAR might in part be explained if one CIMPR molecule bound to two or more of the immobilized uPAR molecules. In addition, the large CIMPR molecule might shield binding epitopes on some of the immobilized uPAR molecules. To elucidate this point, we measured binding of 0.6 μM monoclonal anti-uPAR antibody R4 (K_d 5–10 nM) to the chip with immobilized uPAR. The calculated mole antibody bound per mole uPAR was 0.25 (not shown) indicating some shielding of binding epitopes.

Microdialysis experiments were then performed with ^{125}I-labeled uPAR on one side of the membrane and CIMPR as well as varying concentrations of unlabeled uPAR on both sides. Fig. 4 *B* shows that the binding of uPAR to CIMPR from FCS is saturable with a maximal binding of ~1 mole of uPAR per mole of CIMPR and a K_d of ~11 μM. The result suggests that the lower binding stoichiometry and the higher affinity obtained in the BIAcore experiments is related to the immobilization of uPAR on the sensor chip. In additional experiments, binding of uPAR to CIMPR from bovine and chicken liver were determined from microdialysis experiments each using a single low uPAR concentration. The K_d values were calculated at 8.9 ± 1.9 μM for bovine liver CIMPR and 10 ± 0.7 μM for chicken liver CIMPR (mean values ± 1 SD, n = 5 in each group), in broad agreement with the value obtained for CIMPR from fetal calf serum. In conclusion, the results from experiments using purified receptor preparations show specific binding of uPAR to CIMPR with a Kd in the

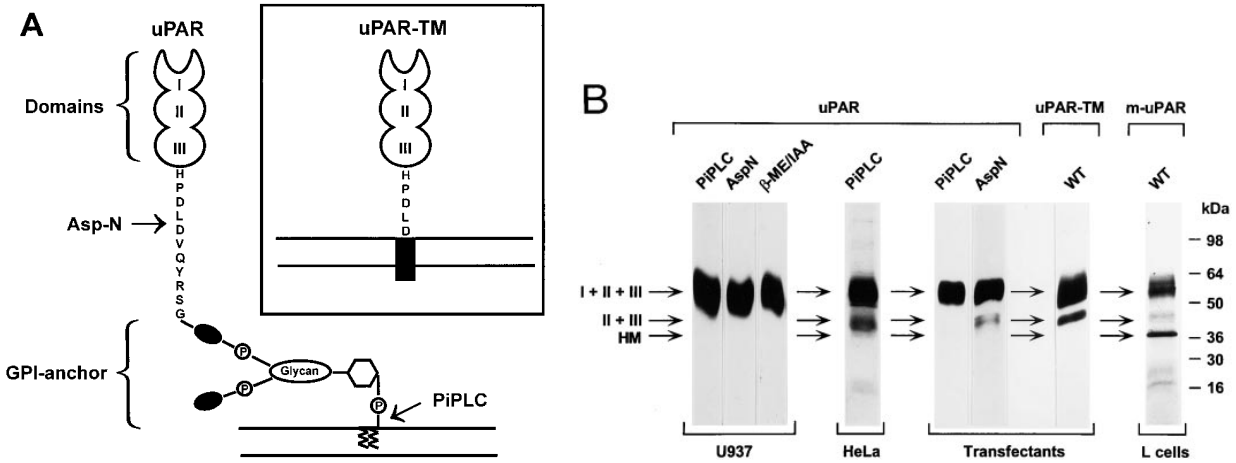

Figure 3. Characterization of labeled uPAR, modified uPAR and m-uPAR. (*A*) Schematic representation explaining the uPAR-TM construct indicating the PiPLC and Asp-N cleavage sites in wild type uPAR. (*B*) SDS-PAGE (8–16%) and fluorography of ^{125}I-uPAR purified from U937 cells, uPAR purified from [^{35}S]methionine/[^{35}S]cysteine-labeled HeLa cells and LB6 clone 19 transfectants expressing wild-type uPAR, and m-uPAR purified from metabolically labeled mouse L cells. Included is also a purified chimeric receptor consisting of domains I + II + III of uPAR linked to the transmembrane domain of the EGF receptor (*uPAR-TM*). Where indicated, uPAR was treated with PiPLC or Asp-N, or reduced and alkylated by β-mercaptoethanol/iodoacetic acid (*βME/IAA*). *Arrows*, migration of uPAR containing all three domains (*I + II + III*), the truncated version containing only domain II + III, and an immature high mannose form of uPAR (*HM form*).

Table I. Characterization of uPAR and m-uPAR Binding to Immobilized CIMPR

Source	uPAR (U937)			uPAR (HeLa)	uPAR transfectant (LB6 cl. 19)		m-uPAR (L cells)	uPAR-TM transfectant
Treatment	PiPLC	Asp-N	PiPLC + β-ME/IAA	PiPLC	PiPLC	Asp-N	None	None
pH 7.2	61.8	64.6	87.8	64.3	72.1	74.3	75.9	73.3
Glc-6-P	2	2.1	3.1	1.4	3	2.1	1.6	4.3
Man-6-P	1.3	2.1	1.4	4.8	2	1.8	1.8	2.5
pH 2.7	35	31.2	5.9	29.5	22.2	21.8	20.8	19.9

The experiments were performed as explained in the legend to Fig. 2 using incubations for 8 min. uPAR purified from U937 cells was ^{125}I labeled, and uPAR from other cellular sources as well as uPAR-TM and m-uPAR were ^{35}S labeled. Treatment with PiPLC or Asp-N, and reduction and alkylation (β-ME/IAA) was performed before the incubation when indicated. The results show the percent of the added radioactivity eluted sequentially in pH 7.2 buffer, in pH 7.2 buffer containing 5 mM Glc-6-P or Man-6-P, and in pH 2.7 buffer. The data are from one of three to seven experiments carried out for each of the ligands.

low micromolar range and with a stoichiometry compatible with a maximal binding of ~1 mol uPAR per mole CIMPR.

Effect of Ligands to uPAR and CIMPR on the Binding Reaction

We then used microdialysis experiments to assess the effect of established ligands to each of the receptors on the binding reaction. Fig. 5 confirms the Man-6-P independent binding of uPAR to CIMPR from FCS at pH 7.4 and the markedly reduced binding at pH 5.5 seen in late endosomes. A similar binding was observed when using bovine or chicken liver CIMPR, whereas no uPAR binding was seen when using irrelevant protein (anti-CIMPR IgG). None of the CIMPR species bound reduced and alkylated uPAR. Catalytically inactivated uPA (DFP-uPA), which binds to uPAR with the same affinity as uPA and pro-uPA, did not influence the binding reaction. On the other hand, the binding was clearly suppressed by β-glucuronidase, which binds to sites in repeats 3 and 9 in CIMPR via Man-6-P epitopes (Dahms et al., 1993). This may suggest a steric hindrance for binding of uPAR to CIMPR occupied with β-glucuronidase. Also, a saturating concentration of IGF-II, which binds to repeat 11 of CIMPR (Dahms et al., 1994; Schmidt et al., 1995) reduced the binding of uPAR. Interestingly, chicken CIMPR does not bind IGF-II (Canfield and Kornfeld, 1989), and uPAR must therefore bind to sites on the receptor different from those that bind IGF-II. Accordingly, IGF-II did not inhibit uPAR binding to chicken liver CIMPR in contrast to the partial inhibition observed when using CIMPR from FCS or bovine liver. We interpret the results to show binding of uPAR to a hitherto unrecognized site on CIMPR that is partially shielded when CIMPR is occupied by β-glucuronidase or IGF-II.

CIMPR in Cells Binds uPAR

To demonstrate binding of endogenous uPAR to CIMPR in cells, metabolically labeled human fibroblasts were incubated in the absence or presence of 5 mM Man-6-P at 4°C and treated with the membrane-impermeable and thiol-cleavable cross-linking reagent DTSSP, followed by solubilization. Cross-linked complexes of uPAR and CIMPR were isolated by immunoprecipitation using Sepharose-coupled anti-uPAR IgG as the first step. This resulted in the precipitation of uPAR, CIMPR, and several other proteins (not shown) as expected in view of the acknowledged binding of uPAR to members of the integrin family. To in-

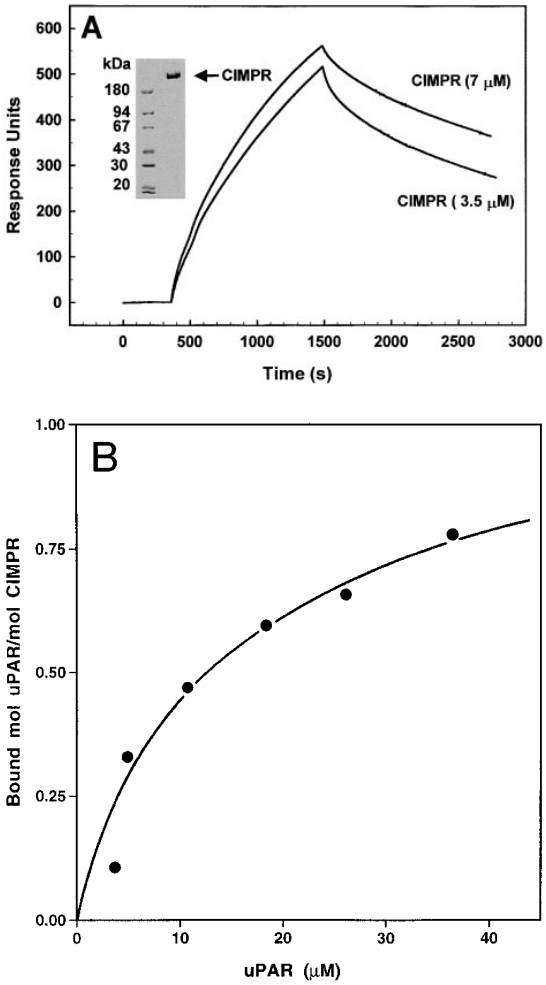

Figure 4. Stoichiometry of uPAR binding to CIMPR. (*A*) Real time interaction analysis was performed by automated measurements of surface plasmon resonance. Sensor chips were either not coupled with protein (flowcell 1) or coupled covalently with pro-uPA (flowcells 2 and 3). Flowcell 3 was superfused with 0.6 μM uPAR expressed in baculovirus, and the number of bound uPAR molecules was calculated after washes. Samples of CIMPR (7 and 3.5 μM) were then applied to flowcell 3 at 20°C using a flow rate of 2 μl/min. The binding reaction was recorded during an injection phase of 1,150 s (starting at 350 s), after which dissociation was measured for the next 1,500 s. The BIAevaluation version 3.0 software was used for the subtraction of the bulk effect of CIMPR. Dissociation of uPAR from pro-uPA was measured separately and subtracted to compensate for drift of the baseline. K_d was calculated at 1.1 μM from the displayed curves, and 0.97 mole of CIMPR was bound to uPAR. The inset shows SDS-PAGE of the CIMPR preparation followed by Coomassie staining. (*B*) Binding was measured by the dialysis exchange method using ^{125}I-labeled uPAR in one chamber only and 25 μM CIMPR in both chambers. Each point represents an experiment in which unlabeled uPAR was present in both chambers at the concentration indicated on the abscissa. The ordinate shows mole of uPAR bound per mole of CIMPR, and the K_d was calculated at 11 μM.

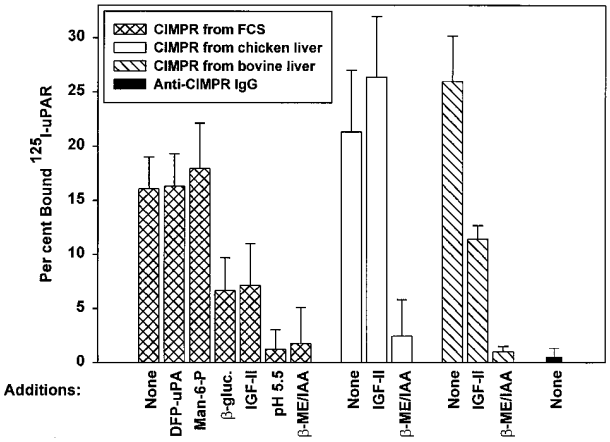

Figure 5. Effect of ligands on binding of uPAR to bovine and chicken CIMPR in solution. Purified CIMPR (3 μM) from FCS (*cross-hatched*), from chicken liver (*open*) or from bovine liver (*hatched*) were applied to both sides of the dialysis membrane. ^{125}I-uPAR (25 pM) was added to one side of the membrane, and competitors were added to both sides. Unless indicated otherwise, the rate of dialysis was measured at pH 7.4, and the percentage of binding was calculated as described in Materials and Methods. Competitors were applied at the following concentrations: Man-6-P, 5 mM; DFP-uPA, 50 nM; β-glucuronidase, 5 μM; IGF-II, 5 μM. When indicated, ^{125}I-uPAR was reduced and alkylated (*β-ME/IAA*) before dialysis. Substitution of CIMPR with anti-CIMPR IgG served as a negative control. The ordinate indicates the calculated percent bound ^{125}I-uPAR, and the bars are the mean values of four to eight determinations ±1 SD.

crease the specificity, a second immunoprecipitation was used, employing anti-CIMPR IgG after release of radioactivity from the Sepharose-coupled anti-uPAR. Finally, the proteins precipitated in the second step were visualized by reducing SDS-PAGE and fluorography. Fig. 6, lanes *1* and *2*, show that uPAR and CIMPR coprecipitated irrespective of presence of Man-6-P in the medium. This result was reproduced in several experiments. Interestingly, both full-length uPAR and the truncated form consisting of DII + DIII were coprecipitated, indicating that the uPA binding domain I of uPAR is not necessary for the interaction. No coprecipitation was observed when Sepharose-coupled anti-uPAR (Fig. 6, lanes *3* and *4*) or anti-CIMPR (not shown) was replaced by irrelevant IgG (anti-LRP). The nature of the ~90-kD protein coprecipitating with uPAR and CIMPR (lanes *1* and *2*) remains unidentified, but may represent a degradation product of CIMPR capable of binding uPAR.

CIMPR Modulates the Subcellular Distribution of uPAR

To elucidate the possible biological role of the interaction between the two receptors, immunofluorescence staining of m-uPAR, by the use of purified anti-uPAR IgG, was performed in permeabilized mouse L cells lacking CIMPR or cells transfected with wild-type or mutated forms of CIMPR. The data shown in Fig. 7 further validate that the anti-uPAR IgG reacts specifically with m-uPAR: ligand blots with the NH_2-terminal fragment of murine urokinase (m-ATF) and Western blots of lysates from murine L cells, and affinity

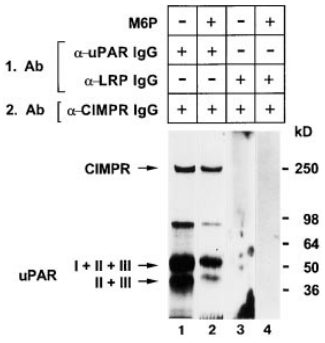

Figure 6. Cross-linking and coimmunoprecipitation of CIMPR and uPAR. Primary cultures of human fibroblasts were metabolically labeled for 18 h with [^{35}S]methionine/[^{35}S]cysteine, and then incubated on ice for 1 h in the absence (lanes *1* and *3*) or presence of 5 mM Man-6-P before cross-linking with 2 mM DTSSP. The cells were solubilized by Triton X-100, and the clarified lysate was immunoprecipitated using Sepharose-coupled, affinity-purified rabbit anti-uPAR IgG (lanes *1* and *2*) or anti LRP (lanes *3* and *4*). The radioactivity was released from the beads at pH 2.5 and reimmunoprecipitated using immobilized rabbit anti-CIMPR IgG. The precipitated material was analyzed by reducing SDS-PAGE (4–16%) and applied to fluorography. The position of molecular size markers are shown to the right.

purification of the lysates using the immobilized anti-uPAR IgG followed by SDS-PAGE and silver staining, gave rise to two or three bands. As visualized by silver staining, the upper band is full-length m-uPAR as it comigrates with the bands obtained by ligand and Western blotting. The middle band, which does not react with m-ATF, is domain II + III (i.e., the truncated form of the receptor lacking the ligand binding domain I), and the lower faint band most likely represents the high mannose form of m-uPAR (Solberg et al., 1992). In other experiments the anti uPAR IgG was used in immunohistochemistry, and labeling was obtained in wild type mouse embryos, but not in m-uPAR knock out embryos (Blasi, F., personal communication).

As demonstrated in Fig. 8, permeabilized CIMPR-negative mouse L cells (clone D9) showed a uniform staining consistent with labeling of m-uPAR on the cell surface (Fig. 8 *a*). By contrast, a punctuate staining consistent with a predominantly vesicular localization of m-uPAR was seen in the cells transfected with wild-type CIMPR (Fig. 8 *b*, *clone Cc2*). Experiments parallel to those shown in Fig. 8, *a* and *b*, but using anti-uPAR IgG preabsorbed to recombinant m-uPAR, did not show any fluorescence (not demonstrated). Culturing of the Cc2 cells in the presence of 400 nM RAP had no influence on the staining pattern

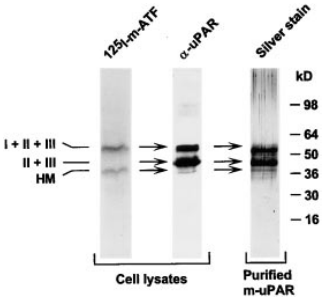

Figure 7. Reaction of purified anti-uPAR IgG with m-uPAR. Lysates of murine L cells were applied to nonreducing SDS-PAGE (8–16%) followed by blotting onto Immobilon membranes and incubation with ^{125}I-labeled NH_2-terminal fragment of mouse uPA (*^{125}I-m-ATF*; *left lane*) or with the purified anti-uPAR IgG (*middle lane*). The right lane shows silver staining of m-uPAR purified from the lysates using Sepharose-coupled anti-uPAR IgG followed by SDS-PAGE and silver staining.

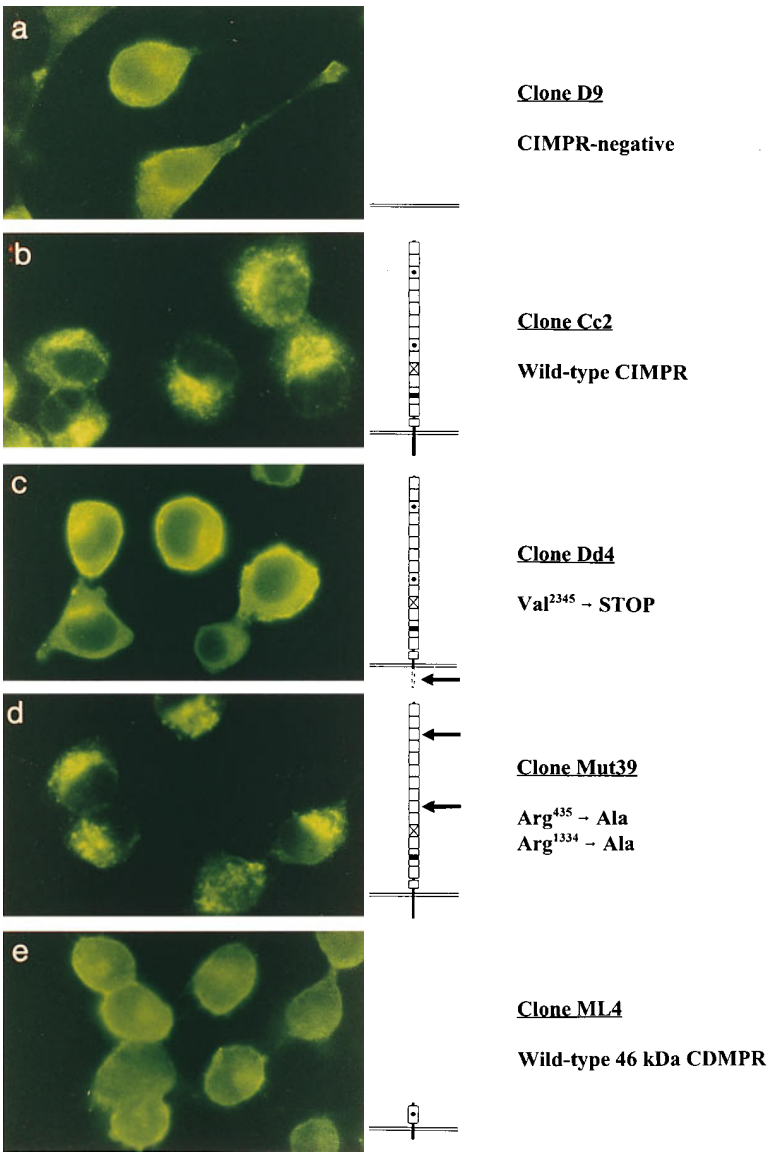

Figure 8. Immunofluorescence of m-uPAR in L cells lacking CIMPR or transfected with different forms of CIMPR. Mouse L cells grown to ~75% confluency were fixed in 3.6% formaldehyde, permeabilized in Triton X-100, and processed for immunofluorescence using affinity-purified rabbit anti-uPAR IgG. The reaction was visualized using a FITC-labeled swine anti–rabbit antibody (*a–e*). Schematic representations of the transfected wild-type or modified CIMPR and of wild-type CDMPR are shown in the right panel. The repeats 3 and 9 of CIMPR with binding sites for Man-6-P are indicated by dots, and the binding site for IGF-II in repeat 11 is indicated by a cross. Mutations and deletions are indicated by arrows. Clone D9 cells are CIMPR-negative control cells; clone Cc2 cells are transfectants encoding wild-type CIMPR; clone Dd4 cells encode a truncated CIMPR lacking the cytoplasmatic tail for endosomal targeting; clone Mut39 cells encode a mutated CIMPR lacking the Man-6-P–binding sites; clone ML4 encodes the 46-kD CDMPR.

(not shown). As shown in Fig. 8 *c*, clone Dd4 cells transfected with a CIMPR lacking the intact sorting signal and impaired in lysosomal sorting (Lobel et al., 1989), exhibited a quite uniform staining for uPAR similar to that of the CIMPR-negative cells. Cells transfected with the clone Mut39 mutant CIMPR incapable of binding Man-6-P ligands as β-glucuronidase (Dahms et al., 1993), showed a staining pattern (Fig. 8 *d*) similar to that of clone Cc2 cells transfected with wild-type CIMPR. This is in accordance with the biochemical data demonstrating Man-6-P–independent binding of uPAR. Finally, the staining pattern in cells transfected with the 46-kD CDMPR was similar to that in the CIMPR-negative cells (Fig. 8 *e*).

Immunoelectron microscopy (Fig. 9) was performed to quantify the subcellular distribution of m-uPAR in the wild-type and transfected cells, and a summary of the results is presented in Table II. Control experiments confirmed that the clone D9 cells did not express CIMPR (not shown). In the D9 cells, ~72% of the endogenous m-uPAR was on the plasma membrane (Fig. 9 *A*), and 28% was in intracellular vesicles. By contrast, in the clone Cc2 cells transfected with wild-type CIMPR, 72% of the uPAR was in intracellular vesicles (Fig. 9 *B*), including small vesicles in the Golgi region (Fig. 9 *B*, *inset*). In the clone Dd4 cells transfected with CIMPR lacking an intact internalization signal, most uPAR was on the cell surface (Fig. 9 *C*) and 39% was intracellular. The clone Mut 39 cells transfected with CIMPR incapable of binding Man-6-P residues exhibited 77% intracellular staining (Fig. 9 *D*) similar to that in the Cc2 cells transfected with wild-type CIMPR. Finally, the clone ML4 cells transfected with the 46-kD receptor showed labeling mainly on the plasma membrane (Fig. 9 *E*) and only 33% intracellular labeling. Thus, the results demonstrate that CIMPR, but not the 46-kD receptor, can modulate the distribution of uPAR in cells via binding to epitopes different from those binding Man-6-P.

CIMPR Targets uPAR to Lysosomes

Double-labeling experiments were first performed to disclose possible colocalization of uPAR and CIMPR in the

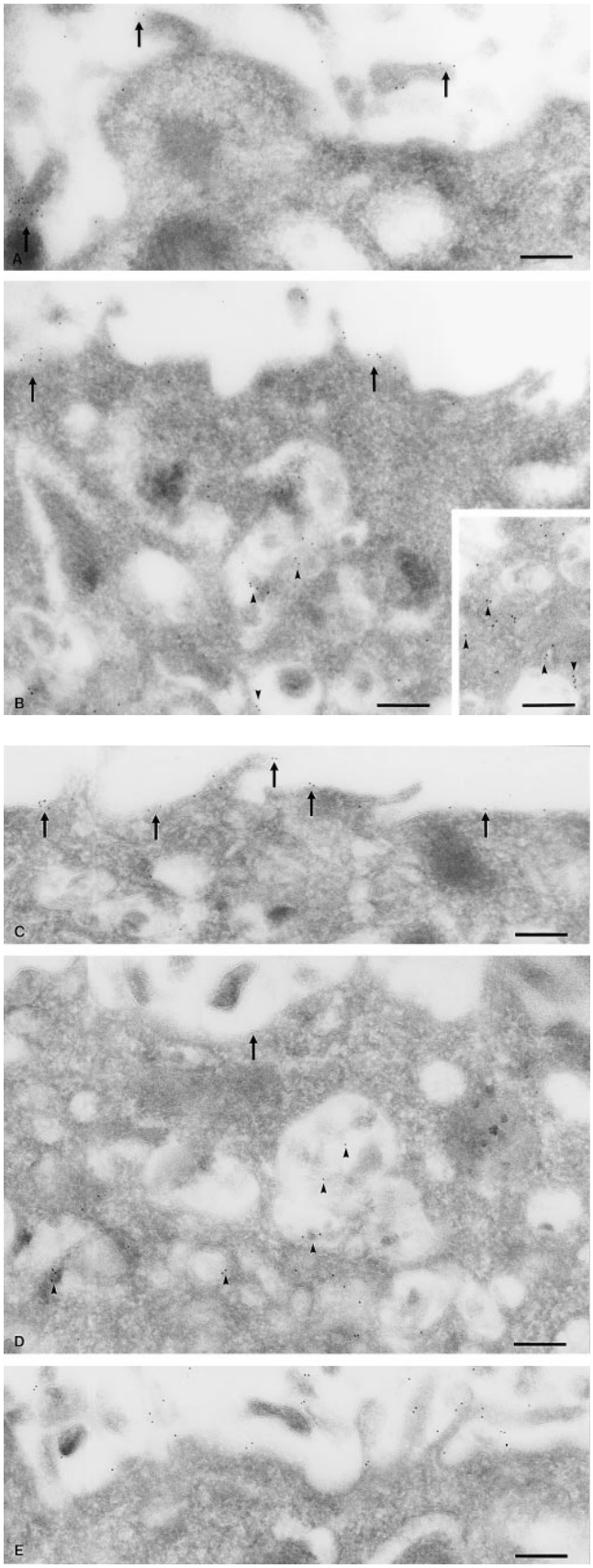

Figure 9. Localization of m-uPAR by immunoelectronmicroscopy. The cells are the same as those used in the immunofluorescence studies. Demonstration of uPAR was performed using 10-nm goat anti–rabbit gold particles. (*A*) Clone D9. Labeling is seen mainly on the plasma membrane including the microvilli (*arrows*). (*B*) Clone Cc2. Labeling is seen on the plasma membrane (*arrows*) and in cytoplasmic vacuoles (*arrowheads*). The inset demonstrates labeling of small Golgi vesicles (*arrowheads*). (*C*) Clone Dd4. Labeling is seen mainly on the plasma membrane (*arrows*). (*D*) Clone Mut39. The labeling is seen in cytoplasmic vacuoles (*arrowheads*). The plasma membrane is indicated by an arrow. (*E*) Clone ML4. Labeling is seen on the plasma membrane. Bar, 0.25 μm.

clone Cc2 cells. Both receptors were colocalized on the cell membrane (Fig. 10 *A*). In vacuoles CIMPR was mainly confined to the endosomal membrane with uPAR distributed throughout the endosomal matrix, and the concentration of uPAR in the vacuoles was greatly increased after treatment of the cells with leupeptin and pepstatin A (Fig. 10 *B*) as compared to untreated cells (not shown). This treatment was used for further analysis of vesicular compartments (Fig. 11 *A*), and double labeling for uPAR and LAMP-2 (Fig. 11 *B*) demonstrates that a large part of the uPAR was in LAMP-2–positive lysosomes.

Discussion

The real time interaction analysis and the microdialysis experiments show that uPAR can bind to CIMPR in a low affinity reaction with a K_d in the low micromolar range and a stoichiometry compatible with ~1 mole uPAR per mole CIMPR. uPAR did not bind to RAP, LRP or IgG used as negative controls, and the binding was abolished after reduction and alkylation of uPAR to disrupt its tertiary structure. In addition, uPAR and CIMPR could be isolated as a complex from ^{35}S-labeled fibroblasts by sequential immunoprecipitation after cross-linking on the cell membrane using a cleavable cross-linker. The coprecipitation of uPAR and CIMPR in the second immunoprecipitation using anti-CIMPR antibody indicated the formation of a true complex between the receptors rather than a cross-linking adduct resulting from random interactions. Firstly, the spacer arm of the cross-linker is 12 Å, which should only allow cross-linking of proteins that are tightly bound to each other. Secondly, control experiments showed no cross-linking between uPAR and the endocytic receptor LRP (Fig. 6, lanes *3* and *4*). This is remarkable since LRP and CIMPR are localized to the same microdomains in the fibroblasts, including coated pits, and since the expression of LRP on the cell surface is estimated to be at least 10 times that of CIMPR (Nykjær, A., unpublished observation). When taken together, these results argue strongly for a specific interaction between uPAR and CIMPR.

The experiments with CIMPR-negative and transfected cells show that CIMPR alter the subcellular distribution of uPAR and targets it to lysosomes. This indicates that the binding interaction studied in vitro reflects a biologically meaningful phenomenon. As both reactants are restricted to a common two dimensional surface in cells, the binding between the highly mobile GPI-anchored uPAR and CIMPR is likely to be more efficient than in solution. It has previously been shown that binding reactions can be

Table II. Distribution of Immunogold Labeling for uPAR in CIMPR-negative and Transfected Cell Lines

Cells	D9	Cc2	Dd4	Mut39	ML4
Plasma membrane	72.1%	27.7%	61.2%	23.0%	67.0%
Intracellular vacuoles	27.9%	72.3%	38.8%	77.0%	33.0%
Total No. of gold particles	756	2,158	1,354	1,198	1,289
Total area, (μm^2)	433.5	261.5	265.5	419	403.5
Gold particles/μm^2	1.74	8.25	5.1	2.9	3.2

Counting of gold particles was performed as described in Materials and Methods. The immunogold labeling on the cell membrane and in intracellular vacuoles are shown in percent of the total number of particles counted.

very efficient when the components are restricted to the same membrane domain. For example, binding of uPA–PAI-1 complex to uPAR greatly facilitates its interaction with LRP in cells (Nykjær et al., 1992). This is due to the association with the cell surface domain, since the ternary complex uPA–PAI-1–uPAR, when studied in soluble form, actually has a lower affinity for LRP than free uPA–PAI-1 complex (Nykjær et al., 1994*a*). It is therefore probable that the interaction between uPAR and CIMPR in cell membranes, because of the two-dimensional arrangement, is more effective than reflected in the low affinities obtained when using the purified components.

The hitherto recognized CIMPR ligands include IGF-II (Morgan et al., 1987) and Man- 6-P–carrying glycoproteins that, in addition to lysosomal enzymes (Lobel, 1987; Kornfeld, 1992), include the propeptide part of the latent TGF-β complex (Purchio et al., 1988; Dennis and Rifkin, 1991; Rifkin et al., 1993; Nunes et al., 1997) and the growth factor proliferin (Lee and Nathans, 1988). The binding site for uPAR on CIMPR is different from that for IGF-II since chicken CIMPR bound uPAR even though it does not bind IGF-II (Canfield and Kornfeld, 1989; Clairmont and Czech, 1989; Zhou et al., 1995). Moreover, the binding of uPAR must occur at site(s) on CIMPR different from those which bind Man-6-P since 5 mM Man-6-P did not inhibit the binding, and since the location of uPAR was similar in cells transfected with wild type CIMPR and the mutant CIMPR lacking intact Man-6-P binding sites. The multifunctional CIMPR therefore harbours at least three different ligand binding sites. Since both β-glucuronidase and IGF-II at high concentrations partially inhibited binding of uPAR, it is possible that the site for uPAR binding is adjacent to or between repeat 11 and repeat 9, which are important for IGF-II and Man-6-P binding, respectively (Dahms et al., 1993, 1994; Schmidt et al., 1995). However, the exact location of segments in CIMPR that are important for binding of uPAR must await future experiments.

The result that CIMPR can target uPAR to lysosomes is in accordance with the previously reported observation in a human breast cancer cell line that uPAR is present in cathepsin D containing vesicles (Bastholm et al., 1994). The present data strongly suggest that uPAR is degraded in the lysosomes since it binds poorly to CIMPR at pH 5.5 and since its concentration in the vesicles is greatly enhanced when using incubations with leupeptin and pepstatin A.

CIMPR is primarily localized in the Golgi and endosomal compartments and is necessary for the efficient transfer of newly synthesized acid hydrolases to lysosomes (Kornfeld, 1992; Pohlmann et al., 1995; Sleat and Lobel, 1997). However, a minor fraction of CIMPR is on the cell surface where it mediates endocytosis and transfer to lysosomes of secreted acid hydrolases, and of IGF-II and other growth factors that are subsequently degraded. In addition, acti-

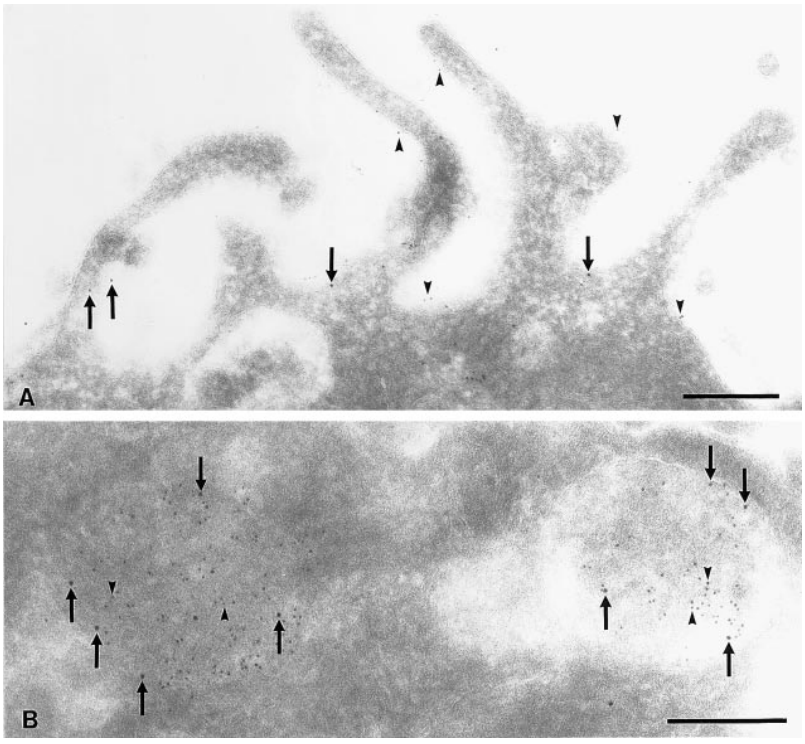

Figure 10. Colocalization of uPAR and CIMPR in Cc2 cells. uPAR, 5-nm gold particles; CIMPR, 10-nm gold particles. (*A*) uPAR (*arrowheads*) and CIMPR (*arrows*) are seen on the plasma membrane, including microvilli. (*B*) Colocalization of uPAR (*arrowheads*) and CIMPR (*arrows*) in late endosomes. The incubation was performed with leupeptin (50 μg/ml) and pepstatin A (67 μg/ml). Bar, 0.25 μm.

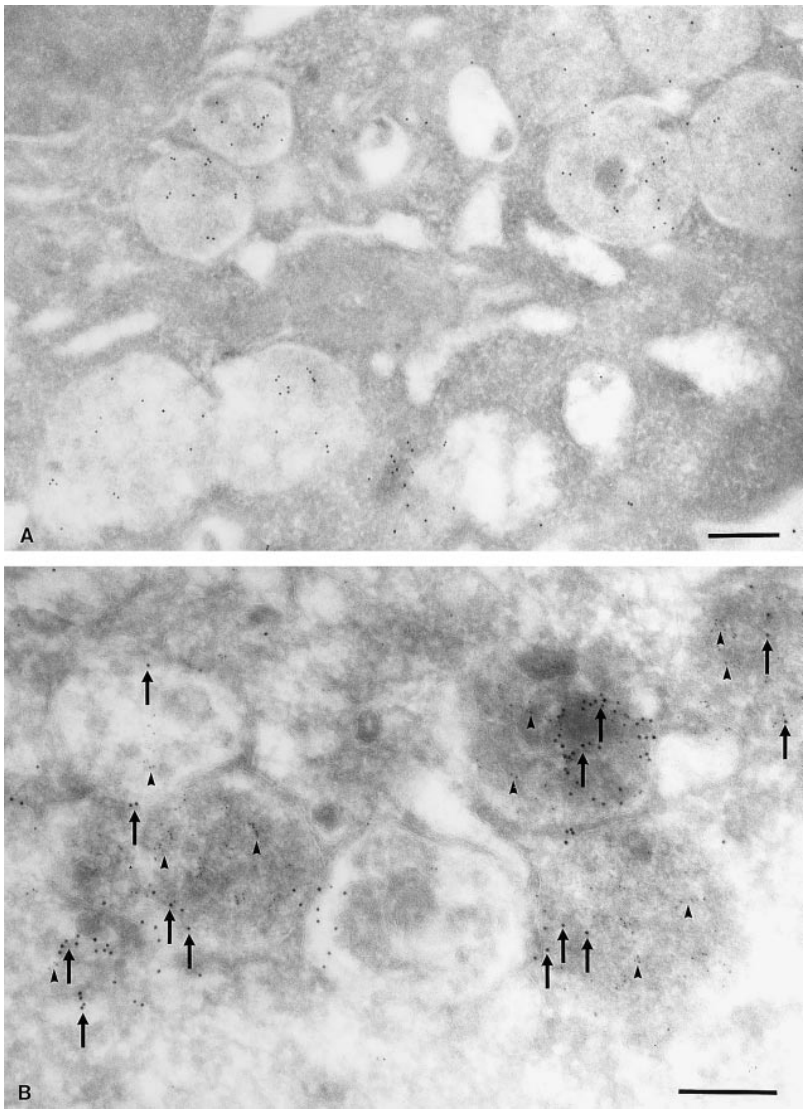

Figure 11. Colocalization of uPAR and LAMP-2 in leupeptin and pepstatin A–treated clone Cc2 cells. uPAR, 5-nm gold particles, LAMP-2, 10-nm gold particles. (*A*) Intense labeling of uPAR in the matrix of electron dense cytoplasmic vacuoles. (*B*) Colocalization of uPAR (*arrowheads*) and the lysosomal marker LAMP-2 (*arrows*). Bar, 0.25 μm.

vation of the latent TGF-β complex at the cell surface is greatly facilitated by binding to CIMPR via the propeptide since the formation of active TGF-β is abrogated by excess Man-6-P or by antibodies that inhibit binding of the latent complex to CIMPR (Dennis and Rifkin, 1991; Rifkin et al., 1993; Nunes et al., 1997). Interestingly, exposure to insulin causes a three- to fourfold increase in the cell surface expression of CIMPR in some cell types (Tanner and Lienhard, 1989), a phenomenon that may contribute to the pleiotropic effects of this hormone. Although not explored in the present experiments, the transfer of uPAR to lysosomes after binding to CIMPR may involve sorting both from the Golgi compartment and from the cell surface. In either case, the result would be a reduction of the cell surface uPAR expression as compared to the LRP-mediated transient downregulation and recycling, which does not lead to disposal of uPAR. It has been shown that ~15% of lysosomal proteins with high affinities for CIMPR and CDMPR escape binding in the Golgi compartment and become secreted into the medium (Kasper et al., 1996). It is likely that a higher fraction of uPAR escapes binding in the Golgi compartment and reaches the cell surface since uPAR has a comparatively low affinity for CIMPR (and does not bind to CDMPR), and since large concentrations of both acid hydrolases and IGF-II may partially inhibit the binding of uPAR. Since the binding of uPAR to CIMPR was not perturbed by uPA, cell surface CIMPR may provide a means for downregulating pericellular proteolysis and cell adhesion by internalization and degradation of uPAR. Interestingly, CIMPR may also provide a clearance pathway for the truncated uPAR consisting of domains DII + DIII after proteolytic removal of DI.

The release of TGF-β from the latent complex depends not only on the expression of CIMPR on the cell surface, but also on the expression of uPAR, which binds uPA and thereby facilitates the activation of plasminogen. Thus, release of active TGF-β is abrogated by inhibition of uPA or plasmin, and cells deficient in uPAR are inefficient in activating the latent complex (Rifkin et al., 1993; Odekon et al., 1994). It may therefore be proposed that CIMPR on the cell surface can assemble both the latent TGF-β complex via binding of Man-6-P epitopes on the TGF-β propeptide and uPAR via sites in domains DII + DIII, and thereby facilitate uPA-mediated generation of plasmin and TGF-β

in the immediate vicinity. According to this hypothesis, increased expression of CIMPR on the cell surface would favor the role of uPAR in generation of the growth inhibitor TGF-β, which can reduce migratory ability (Irving and Lala, 1995) as opposed to the initiation of pericellular proteolytic cascades. In addition, it is possible that interaction of domains DII + DIII with uPAR may perturb their binding to vitronectin. This setting may, together with the degradation of the mitogen IGF-II that can stimulate cell migration by yet unknown mechanisms (Irving and Lala, 1995), contribute to the role of CIMPR in control of cell growth and migration. Interestingly, expression of CIMPR is reduced in both rat and human hepatocarcinomas (Sue et al., 1995). In addition, it has been postulated that CIMPR functions as a tumor suppressor in human liver carcinogenesis since frequent loss of heterozygosity occurs at the CIMPR locus and since accompanying mutations in the remaining allele resulting in truncated CIMPR have been demonstrated (De Souza et al., 1995; Yamada et al., 1997). The present results suggest that deranged function of uPAR resulting from lack of CIMPR may play a contributing role in the carcinogenesis. Future studies should show whether CIMPR has a general impact in modulating the role of uPAR in cell migration and invasion.

In conclusion, we have shown that CIMPR can bind uPAR via a previously unrecognized binding site and modulate the distribution of uPAR in cells, and we propose that this interaction contributes to the regulation of the multitude of uPAR functions.

We thank Dr. C. Jacobsen for valuable help in performing real time interaction analysis. Drs. S. Carlsson, N.M. Dahms, I. Mellman, E. Rønne, W. Sly, and R.F. Todd III are thanked for reagents. S. Andersen, I. Kristoffersen, and H. Sidelmann are acknowledged for excellent technical assistance.

This work was supported by grants from the Danish Biomembrane Research Center (to A. Nykjær, E.I. Christensen, and J. Gliemann), Danish Cancer Society (to J. Gliemann), Danish Medical Research Council (to A. Nykjær, E.I. Christensen, J. Gliemann), Lysgaard Foundation (to A. Nykjær), Carlsberg Foundation (to A. Nykjær), and Novo Nordisk Foundation (E.I. Christensen, J. Gliemann).

References

Andreasen, P.A., L. Kjøller, L. Christensen, and M.J. Duffy. 1997. The urokinase-type plasminogen activator system in cancer metastases. A review. *Int. J. Cancer*. 72:1–22.

Bastholm, L., F. Elling, N. Brunner, and M.H. Nielsen. 1994. Immunoelectron microscopy of the receptor for urokinase plasminogen activator, and cathepsin D in the human breast cancer cell line MDA-MB-231. *APMIS.* 102:279–286.

Behrendt, N., E. Rønne, and K. Danø. 1996. Domain interplay in the urokinase receptor. Requirements for the third domain in high affinity ligand binding and demonstration of ligand contact sites in distinct receptor domains. *J. Biol. Chem*. 271:22885–22894.

Bohuslav, J., V. Horejsi, C. Hansmann, J. Stöckl, U.H. Weidle, O. Majdic, I. Bartke, W. Knapp, and H. Stockinger. 1995. Urokinase plasminogen activator, β2-integrins, and Src-kinases within a single receptor complex of human monocytes. *J. Exp. Med.* 181:1381–1390.

Brunetti, C.R., R.L. Burke, S. Kornfeld, W. Gregory, F.R. Masiarz, K.S. Dingwell, and D.C. Johnson. 1994. Herpes simplex virus glycoprotein D acquires mannose 6-phosphate residues and binds to mannose 6-phosphate receptors. *J. Biol. Chem.* 269:17067–17074.

Bugge, T.H., T.T. Suh, M.J. Flick, C.C. Daugherty, J. Rømer, H. Solberg, V. Ellis, K. Danø, and J.L. Degen. 1995. The receptor for urokinase-type plasminogen activator is not essential for mouse development or fertility. *J. Biol. Chem.* 270:16886–16894.

Busso, N., S.K. Masur, D. Lazega, S. Waxman, and L. Ossowski. 1994. Induction of cell migration by pro-urokinase binding to its receptor: Possible mechanisms for signal transduction in human epithelial cells. *J. Cell Biol.* 126:259–270.

Canfield, W.M., and S. Kornfeld. 1989. The chicken liver mannose 6-phosphate receptor lacks the high affinity binding site for insulin-like growth factor II. *J. Biol. Chem.* 264:7100–7103.

Chapman, H.A. 1997. Plasminogen activators, integrins, and the coordinated regulation of cell adhesion and migration. *Curr. Opin. Cell Biol.* 9:714–724.

Clairmont, K.B., and M.P. Czech. 1989. Chicken and xenopus mannose 6-phosphate receptors fail to bind insulin-like growth factor II. *J. Biol. Chem.* 264: 16390–16392.

Conese, M., A. Nykjær, C.M. Petersen, O. Cremona, R. Pardi, P.A. Andreasen, J. Gliemann, E.I. Christensen, and F. Blasi. 1995. α2-macroglobulin receptor/LDL receptor-related protein (LRP)-dependent internalization of the urokinase receptor. *J. Cell Biol*. 131:1609–1622.

Cubellis, M.V., T.C. Wun, and F. Blasi. 1990. Receptor-mediated internalization and degradation of urokinase is caused by its specific inhibitor PAI-1. *EMBO (Eur. Mol. Biol. Organ.) J.* 9:1079–1085.

Dahms, N.M., P.A. Rose, J.D. Molkentin, Y. Zhang, and M.A. Brzycki. 1993. The bovine mannose 6-phosphate/insulin-like growth factor II receptor. The role of arginine residues in mannose 6-phosphate binding. *J. Biol. Chem.* 268:5457–5463.

Dahms, N.M., D.A. Wick, and M.A. Brzycki-Wessell. 1994. The bovine mannose 6-phosphate/insulin-like growth factor II receptor. Localization of the insulin-growth factor II binding site to domains 5-11. *J. Biol. Chem.* 269: 3802–3809.

Deng, G., S.A. Curriden, S. Wang, S. Rosenberg, and D.J. Loskutoff. 1996. Is plasminogen activator inhibitor-1 the molecular switch that governs urokinase receptor-mediated cell adhesion and release? *J. Cell Biol*. 134:1563–1571.

Dennis, P.A., and D.B. Rifkin. 1991. Cellular activation of latent transforming growth factor β requires binding to the cation-independent mannose 6-phosphate/insulin-like growth factor type II receptor. *Proc. Natl. Acad. Sci. USA.* 88:580–584.

De Souza, A.T., G.R. Hankins, M.K. Washington, T.C. Orton, and R.L. Jirtle. 1995. Man-6-P/IGF2R gene is mutated in human hepatocellular carcinomas with loss of heterozygosity. *Nat. Genet.* 11:447–449.

Ellis, V., M.F. Scully, and V.V. Kakkar. 1989. Plasminogen activation initiated by single-chain urokinase-type plasminogen activator. Potentiation by U937 monocytes. *J. Biol. Chem.* 264:2185–2188.

Estreicher, A., J. Mühlhauser, J. Carpentier, J.-L. Orci, and J.-D. Vassali. 1990. The receptor for the urokinase type plasminogen activator polarizes expression of the protease to the leading edge of migrating monocytes and promotes degradation of enzyme inhibitor complexes. *J. Cell Biol.* 111:783–792.

Fazioli, F., and F. Blasi. 1994. Urokinase-type plasminogen activator and its receptor: new targets for anti-metastatic therapy? *Trends Pharmacol. Sci.* 15: 25–29.

Griffiths, G., A. McDowall, R. Back, and J. Dubochet. 1984. On the preparation of cryosections for immunocytochemistry. *J. Ultrastruct. Res.* 89:65–78.

Heegaard, C.W., A.C. Simonsen, K. Oka, L. Kjøller, A. Christensen, B. Madsen, L. Ellgaard, L. Chan, and P.A. Andreasen. 1995. Very low density lipoprotein receptor binds and mediates endocytosis of urokinase-type plasminogen activator type-1 plasminogen activator inhibitor complex. *J. Biol. Chem.* 270:20855–20861.

Hoflack, B., and S. Kornfeld. 1985. Purification and characterization of a cation-dependent mannose 6-phosphate receptor from murine P388D1 macrophages and bovine liver. *J. Biol. Chem.* 260:12008–12014.

Høyer-Hansen, G., E. Rønne, H. Solberg, N. Behrendt, M. Plough, L.R. Lund, V. Ellis, and K. Danø. 1992. Urokinase plasminogen activator cleaves its cell surface receptor releasing the ligand-binding domain. *J. Biol. Chem.* 267: 18224–18229.

Irving, J.A., and P.K. Lala. 1995. Functional role of surface integrins on human trophoblast cell migration: Regulation by TGF-β, IGF-II, and IGFBP-1. *Exp. Cell Res.* 217:419–427.

Jadot, M., W.M. Canfield, W. Gregory, and S. Kornfeld. 1992. Characterization of the signal for rapid internalization of the bovine mannose 6-phosphate/insulin-like growth factor II receptor. *J. Biol. Chem.* 267:11069–11077.

Jensen, P.H., E.I. Christensen, P. Ebbesen, J. Gliemann, and P.A. Andreasen. 1990. Lysosomal degradation of receptor-bound urokinase-type plasminogen activator is enhanced by its inhibitors in human trophoblastic choriocarcinoma cells. *Cell Regul*. 1:1043–1056.

Johnson, K.F., W. Chan, and S. Kornfeld. 1990. Cation-dependent mannose 6-phosphate receptor contains two internalization signals in its cytoplasmatic domain. *Proc. Natl. Acad. Sci. USA.* 87:10010–10014.

Kanse, S.M., C. Kost, O.G. Wilhelm, P.A. Andreasen, and K.T. Preissner. 1996. The urokinase receptor is a major vitronectin-binding protein on endothelial cells. *Exp. Cell Res.* 224:344–353.

Kasper, D., F. Dittmer, K. von Figura, and R. Pohlmann. 1996. Neither type of mannose 6-phosphate receptor is sufficient for targeting of lysosomal enzymes along intracellular routes. *J. Cell Biol.* 134:615–623.

Kjøller, L., S.M. Kanse, T. Kirkegaard, K.W. Rodenburg, E. Rønne, S.L. Goodman, K.T. Preissner, L. Ossowski, and P.A. Andreasen. 1997. Plasminogen activator inhibitor-1 represses integrin- and vitronectin-mediated cell migration independently of its function as an inhibitor of plasminogen activation. *Exp. Cell. Res.* 232:420–429.

Kornfeld, S. 1992. Structure and function of the mannose 6-phosphate/insulin-like growth factor receptors. *Annu. Rev. Biochem.* 61:307–330.

Lee, S.J., and D. Nathans. 1988. Proliferin secreted by cultured cells binds to mannose 6-phosphate receptors. *J. Biol. Chem.* 263:3521–3537.

Lobel, P., N.M. Dahms, J. Breitmeyer, J.M. Chirgwin, and S. Kornfeld. 1987.

Cloning of the bovine 215-kDa cation-independent mannose 6-phosphate receptor. *Proc. Natl. Acad. Sci. USA*. 84:2233–2237.
Lobel, P., K. Fujimoto, R.D. Ye, G. Griffith, and S. Kornfeld. 1989. Mutations in the cytoplasmic domain of the 275 kd mannose 6-phosphate receptor differentially alter lysosomal enzyme sorting and endocytosis. *Cell.* 57:787–796.
Ludwig, T., G. Griffith, and B. Hoflack. 1991. Distribution of newly synthesized lysosomal enzymes in the endocytic pathway of normal rat kidney cells. *J. Cell Biol.* 115:1561–1572.
Masucci, M-T., N. Pedersen, and F. Blasi. 1991. A soluble, ligand binding mutant of the human urokinase plasminogen activator receptor. *J. Biol. Chem.* 266:8655–8658.
Mizukami, I.F., S.D. Vinjamuri, F. Perini, E.D.Y. Liu, and R.F. Todd III. 1991. Purification, biochemical composition, and biosynthesis of the Mo3 activation antigen expressed on the plasma membrane of human mononuclear cells. *J. Immunol.* 147:1331–1337.
Moestrup, S.K., and J. Gliemann. 1991. Analysis of ligand recognition by the purified alpha 2-macroglobulin receptor (low density lipoprotein receptor-related protein). *J. Biol. Chem.* 266:14011–14017.
Møller, L.B., M. Ploug, and F. Blasi. 1992. Structural requirements for glycosylphosphatidylinositol-anchor attachment in the cellular receptor for urokinase plasminogen activator. *Eur. J. Biochem.* 208:493–500.
Morgan, D.O., J.C. Edman, D.N. Standring, V.A. Fried, M.C. Smith, R.A. Roth, and W.J. Rutter. 1987. Insulin-like growth factor II as a multifunctional binding protein. *Nature.* 329:301–307.
Nunes, I., P.E. Gleizes, C.N. Metz, and D.B. Rifkin. 1997. Latent transforming growth factor-binding protein domains involved in activation and transglutaminase-dependent cross-linking of latent transforming growth factor-β. *J. Cell Biol.* 136:1151–1163.
Nykjær, A., C.M. Petersen, B. Møller, P.H. Jensen, S.K. Moestrup, T.L. Holtet, M. Etzerodt, H.C. Thøgersen, M. Munch, P.A. Andreasen, and J. Gliemann. 1992. Purified alpha 2-macroglobulin receptor/LDL receptor-related protein binds urokinase:plasminogen activator inhibitor type-1 complex. Evidence that the alpha 2-macroglobulin receptor mediates cellular degradation of urokinase receptor-bound complexes. *J. Biol. Chem.* 267:14543–14546.
Nykjær, A., G. Bengtsson-Olivecrona, A. Lookene, S.K. Moestrup, C.M. Petersen, W. Weber, U. Beisiegel, and J. Gliemann. 1993. The alpha 2-macroglobulin receptor/low density lipoprotein receptor-related protein binds lipoprotein lipase and beta-migrating very low density lipoprotein associated with the lipase. *J. Biol. Chem.* 268:15048–15055.
Nykjær, A., L. Kjøller, R.L. Cohen, D.A. Lawrence, B.A. Garni-Wagner, R.F. Todd III, A-J. van Zonneveld, J. Gliemann, and P.A. Andreasen. 1994*a*. Regions involved in binding of urokinase-type-1 inhibitor complex and prourokinase to the endocytic α2-macroglobulin receptor/low density lipoprotein receptor-related protein. *J. Biol. Chem.* 269:25668–25676.
Nykjær, A., B. Møller, R.F. Todd III, T. Christensen, P.A. Andreasen, J. Gliemann, and C.M. Petersen. 1994*b*. Urokinase receptor. An activation antigen in human T lymphocytes. *J. Immunol.* 152:505–516.
Nykjær, A., M. Conese, E.I. Christensen, D. Olson, O. Cremona, J. Gliemann, and F. Blasi. 1997. Recycling of the urokinase receptor upon internalization of the uPA: serpin complexes. *EMBO (Eur. Mol. Biol. Organ.) J.* 16:2610–2620.
Odekon, L.E., F. Blasi, and D.B. Rifkin.1994. Requirement for receptor-bound urokinase in plasmin-dependent cellular conversion of latent TGF-β to TGF-β. *J. Cell. Physiol.* 158:398–407.
Pedersen, A.O., B. Hust, S. Andersen, F. Nielsen, and R. Brodersen. 1986. Laurate binding to human serum albumin. Multiple binding equilibria investigated by a dialysis exchange method. *Eur. J. Biochem.* 154:445–552.
Pohlmann, R., M.W. Boeker, and K. von Figuira. 1995. The two mannose 6-phosphate receptors transport distinct complements of lysosomal enzymes. *J. Biol. Chem.* 270:27311–27318.
Purchio, A.F., J.A. Cooper, A.M. Brunner, M.N. Lioubin, L.E. Gentry, K.S. Kovachina, R.A. Roth, and H. Marquardt. 1988. Identification of mannose 6-phosphate in two asparagine-linked sugar chains of recombinant transforming growth factor β1 precursor. *J. Biol. Chem.* 263:14211–14215.
Resnati, M., M. Guttinger, S. Valcamonica, N. Sidenius, F. Blasi, and F. Fazioli. 1996. Proteolytic cleavage of the urokinase receptor substitutes for the agonist-induced chemotactic effect. *EMBO (Eur. Mol. Biol. Organ.) J.* 15:1572–1582.
Rifkin, D.B, S. Kojima, M. Abe, and J.G. Harpel. 1993. TGF-β: structure, function, and formation. *Thromb. Haemostasis.* 70:177–179.
Roldan, A.L., M.V. Cubellis, M.T. Masucci, N. Behrendt, L.R. Lund, K. Danø, E. Appella, and F. Blasi. 1990. Cloning and expression of the receptor for human urokinase plasminogen activator, a central molecule in cell surface, plasmin dependent proteolysis. *EMBO (Eur. Mol. Biol. Organ.) J.* 9:467–474.
Schmidt, B., C. Kiecke-Siemsen, A. Waheed, T. Braulke, and K. von Figura. 1995. Localization of the insulin-like growth factor II binding site to amino acids 1508-1566 in repeat 11 of the mannose 6-phosphate/insulin-like growth factor II receptor. *J. Biol. Chem.* 270:14975–14982.
Simon, D.I., N.K. Rao, H. Xu, Y. Wei, O. Majdic, E. Rønne, L. Kobzik, and H.A. Chapman. 1996. Mac-1 (CD11b/CD18) and the urokinase receptor (CD87) form a functional unit on monocytic cells. *Blood*. 88:3185–3194.
Sleat, D.E., and P. Lobel. 1997. Ligand binding specificities of the two mannose 6-phosphate receptors. *J. Biol. Chem.* 272:731–732.
Solberg, H., D. Løber, J. Eriksen, M. Ploug, E. Rønne, N. Behrendt, K. Danø, and G. Høyer-Hansen. 1994. Identification and characterization of the murine cell surface receptor for the urokinase-type plasminogen activator. *Eur. J. Biochem.* 205:451–458.
Solberg, H., J. Rømer, N. Brunner, A. Holm, N. Sidenius, K. Danø, and G. Høyer-Hansen. 1994. A cleaved form of the receptor for urokinase-type plasminogen activator in invasive transplanted human and murine tumors. *Int. J. Cancer*. 58:877–881.
Stefansson, S., and D.A. Lawrence. 1996. The serpin PAI-1 inhibits cell migration by blocking integrin αVβ3 binding to vitronectin. *Nature.* 383:441–443.
Sue, S.R., R.S. Chari, F.M. Kong, J.J. Mills, R.L. Fine, R.L. Jirtle, and W.C. Meyers. 1995. Transforming growth factor-beta receptors and mannose 6-phosphate/insulin growth factor-II receptor expression in human hepatocellular carcinoma. *Ann. Surg.* 222:171–178.
Tanner, L.I., and G.E. Lienhard. 1989. Localization of transferrin receptors and isulin-like growth factor II receptors in vesicles from 3T3-L7 adipocytes that contain intracellular glucose transporters. *J. Cell Biol.* 108:1537–1545.
Tokuyasu, K.T. 1978. A study of positive staining of ultrathin frozen sections. *J. Ultrastruct. Res.* 63:287–307.
Yamada, T., A.T. De Souza, S. Finkelstein, and R.L. Jirtle. 1997. Loss of the gene encoding mannose 6-phosphate/insulin-like growth factor II receptor is an early event in liver carcinogenesis. *Proc. Natl. Acad. Sci. USA*. 94:10351–10355.
Weaver, A.M., I.M. Hussaini, A. Mazar, J. Henkin, and S.L. Gonias. 1997. Embryonic fibroblasts that are genetically deficient in low density lipoprotein receptor-related protein demonstrate increased activity of the urokinase receptor system and accelerated migration on vitronectin. *J. Biol. Chem*. 272: 14372–14379.
Wei, Y., D.A. Waltz, N. Rao, R.J. Drummond, S. Rosenberg, and H.A. Chapman. 1994. Identification of the urokinase receptor as an adhesion receptor for vitronectin. *J. Biol. Chem.* 269:32380–32388.
Wei, Y., M. Lukashev, D.I. Simon, S.C. Bodary, S. Rosenberg, M.V. Doyle, and H.A. Chapman. 1996. Regulation of integrin function by the urokinase receptor. *Science.* 273:1551–1555.
Zhou, M., Z. Ma, and W.S. Sly. 1995. Cloning and expression of the cDNA of chicken cation-independent mannose-6-phosphate receptor. *Proc. Natl. Acad. Sci. USA*. 92:9762–9766.